Plume Modeling of a Two CAMILA Hall Thruster Cluster for Thrust Vectoring

IEPC-2015-71／ISTS-2015-b-71

Presented at Joint Conference of 30th International Symposium on Space Technology and Science, 34th International Electric Propulsion Conference and 6th Nano-satellite Symposium
Hyogo-Kobe, Japan
July 4–10, 2015

Matteo Laterza * and Moshe Guelman†
Technion - Israeli Institute of Technology, Haifa, 32000, Israel

The present work focuses on plume interactions in a convergent Hall thruster cluster for thrust vectoring. The analysis is done through a numerical model, using a custom hybrid-PIC code with Monte Carlo Collisions for ion-neutral interactions. The setup consists in two thrusters positioned at $10cm$ separation, each with a 10^o convergence angle. In order to provide thrust vectoring, the ion current is changed by $\pm 20\%$ relatively to nominal. A combined simulation is compared with stand-alone simulations of the two thrusters. The comparison shows not only the deflection of high-angle charge-exchange ions, but also deviations of the main plume. A non-axisymmetric divergence model is developed, showing total divergence on the convergence plane to be smaller than single thruster divergence, contrary to what would be expected.

Nomenclature

B	= magnetic field
e	= electron charge (absolute value)
j	= specific current
K_b	= Boltzmann constant
n	= number density
$P(j)$	= current probability distribution function on sampling surface
R	= sampling radius
T_e	= electron temperature
v	= ion velocity
ϕ	= plasma potential

*Doctoral student, Department of Aerospace Engineering, mlaterza@tx.technion.ac.il .
†Professor emeritus, Department of Aerospace Engineering, aerglmn@tx.technion.ac.il .

I. Introduction

The Co-Axial Magnetically Insulated Long-Anode Hall Thruster (CAMILA) developed at Technion has proven to have a very high performance for its class;[1] opening a wide range of possible applications.[2] Before implementing this thruster on a space system, however, a detailed analysis of its plume is necessary. As today, in fact, only the acceleration channel and the physical processes involved have been studied extensively.[3,4] Some studies have been done on the near field plume,[5] but more are necessary.

The present study focuses on the interaction of the plumes of two CAMILA Hall thrusters in a converging thrust-vectoring configuration.

A converging channel configuration for thrust vectoring with Hall thrusters was proposed by Snecma and CNES.[6] Their configuration was a "multichannel" thruster, with the acceleration channels sharing a common cathode, power supply and magnetic circuit. In their research it was shown that thrust vectoring by converging channels was a viable option, but convergence angles exceeding $10^o \div 20^o$ were discouraged on the basis of an expected larger divergence and erosion. These predictions were however based on the assumption that the plumes would be unaffected by each other.

Extensive experimental and numerical studies on the plume interactions of clusters of Hall thrusters have been carried out in numerous institutions, most noticeably by Gallimore, Beal, Walker and Hargus at University of Michigan.[7,8] These studies proved that cluster plumes are predictable from single thruster data. One of the most interesting results, however, is that the plume divergence of the cluster is slightly smaller than what would be expected from single thruster plume superposition. The phenomenon was explained with the deviation of slow charge-exchange ions by the higher potential of the plume cores. All these studies, however, were based on thrusters positioned with their axes of symmetry parallel to each other.

By analyzing, through a numerical model, the interactions of the plumes in a converging cluster, we aim to shed light on the potential of this thrust vectoring configuration, and especially on the effect of convergence on plume divergence and charge-exchange ion trajectories.

II. Numerical Model

A. General Model

The region of interest is the far-field plume, where the magnetic field is negligible. The size of the computational domain is on the order-of-magnitude of the meter and there is no interaction with solid surfaces. The model that best fits those characteristics is a hybrid-Particle-In-Cell, where heavy species are considered as particles and electrons are considered as fluid.

The ion number density is computed by scattering the positions of macroparticles representing ions on a computational grid. Quasi-neutrality is assumed, and electron number density is considered equal as ion. Electron temperature is computed using a polytropic expansion:

$$T_e = T_{e0} \left(\frac{n}{n_0} \right)^{\gamma - 1} \tag{1}$$

The index $_0$ indicates the reference values given as input. The coefficient γ can vary between 1 for an isothermal expansion to 5/3 for an adiabatic one. The used value of 1.2 is taken from literature[9] waiting for experimental data.

Using the assumption of quasi-neutrality we can compute the electric potential by inserting Eq.1 in the inverted Boltzmann relation to obtain:

$$\phi = \phi_0 - \frac{K_b T_e}{e} \frac{1 - \left(\frac{n}{n_0} \right)^{\gamma - 1}}{\gamma - 1} \tag{2}$$

The electric field is then computed with the central differences method and used to update the velocity and position of ion macroparticles using the leapfrog method[10] .

Ions from different thrusters and different species are stored separately, in order to be able to compare the behavior of a thruster in the combined simulation with the one of a thruster simulated stand-alone.

When steady-state is reached, field data are averaged over a number of cycles in order to have better statistical data.

B. Collisions

The relevant collisions for the density and energy levels typical of the CAMILA plume are ion-neutral charge-transfer and momentum-transfer collisions.[4] A simple Monte Carlo Collisions model is used. The neutral number density distribution is pre-computed using the same computational model.

Post-collision velocities are computed using statistical sampling from a differential cross-section distribution. The collision model was tested on a simulation where a parallel beam of ions hits a neutral target. Figure 1 shows charge-exchange and momentum-transfer ions post collision positions and velocities, while Fig.2 shows the comparison between the computed differential cross-sections and the literature data[11] .

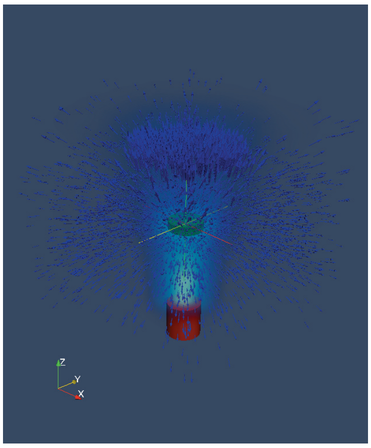

Figure 1: Collision testing configuration. Ion emitter in red, target in green.

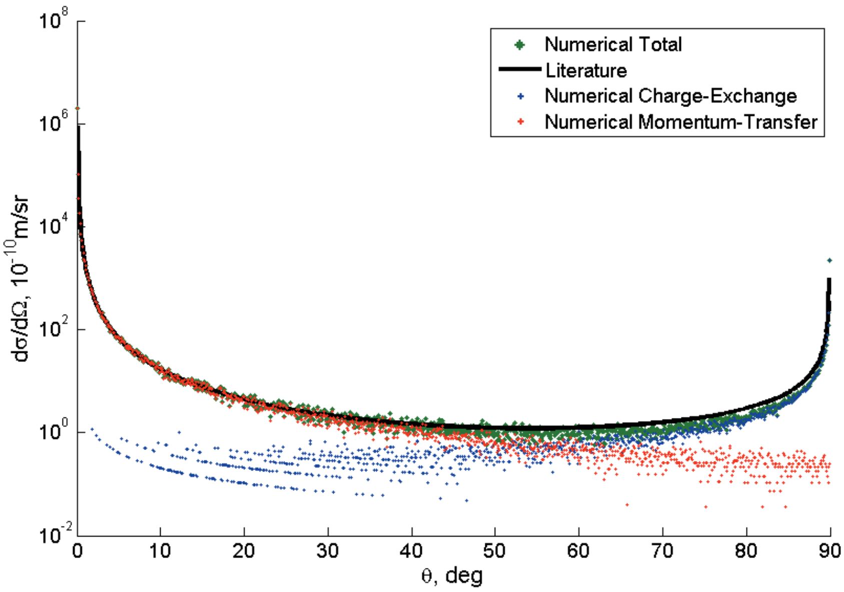

Figure 2: Comparison between literature data for ion-neutral differential cross-sections and collision test.

III. Simulations

A. Setting

The simulated cluster is composed by two thrusters, with a distance between the centers of the exit planes of $0.1m$. Both thrusters have a convergence angle of 10^o, with a total angle between their symmetry axes of 20^o. The two thrusters are set at different mass flow rates, one 20% above nominal value and the other 20% below. Ionization rates and ion velocities are assumed to be constant, so the ion current is proportional to the mass flow. Figure 3 shows the domain geometry. The center point of the two thrusters is at the axes origin, and the domain spans between $-0.4m$ and $0.4m$ on the x and y directions, and from 0 to $1m$ in the z direction. The thruster symmetry axes lay on the xz plane.

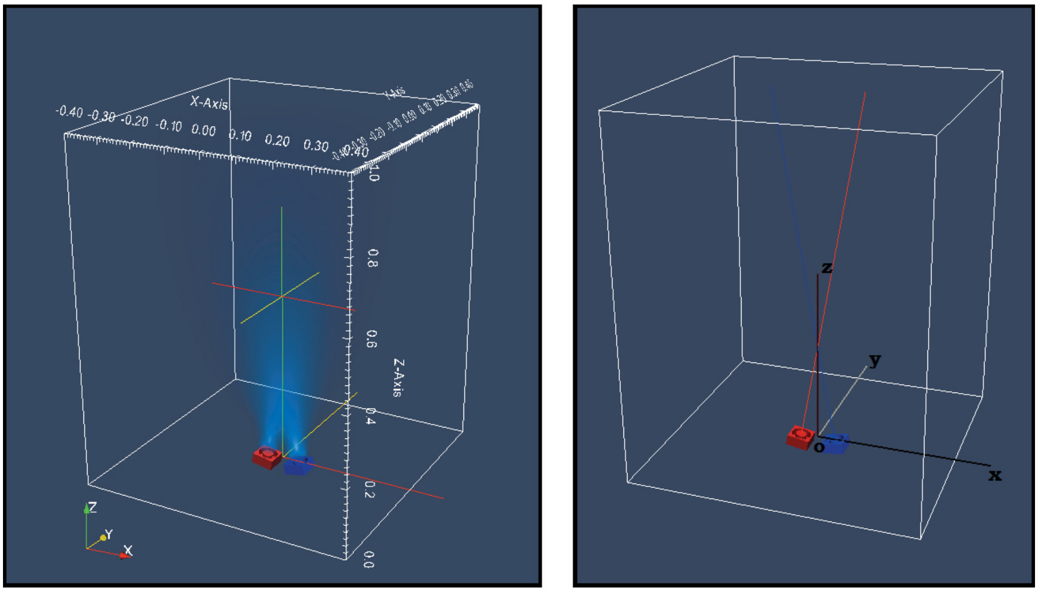

Figure 3: Thruster positioning inside the computational domain. High flux thruster is represented on the right in blue, low flux on the left in red.

Three simulations are performed: one combined simulation in which both thrusters are fired together and two stand-alone simulations in which the thrusters are fired separately.

Table 1 summarizes the various simulation parameters.

Table 1: Simulation parameters.

General		Thruster	Low Flux	High Flux
Mesh size	$5mm$	Mass flow ratio	80% nominal	120% nominal
Time step	2×10^{-7}s	y rotation	-10^o	10^o
x span	$-0.4 \div 0.4m$	Center x position	$-0.05m$	$0.05m$
y span	$-0.4 \div 0.4m$	Real-to-computational number ratio	1×10^8	1×10^8
z span	$0 \div 1m$			

B. Input

The simulation input is mainly based on channel and near-field experimental data.[5] The first operation was to chose a sampling surface where to interface the input data with the simulation. The main sampling plane must be positioned at a distance from the channel exit big enough to be outside the potential fall caused by the magnetization of the electrons.[12] Figure 4 shows the selection of the sampling plane at $z = 6mm$

in thruster coordinates. A cylindrical surface is added at $r = 33mm$ in order to capture the high-angle charge-exchange ions. Figure 5 shows the sampling profile in thruster rz coordinates.

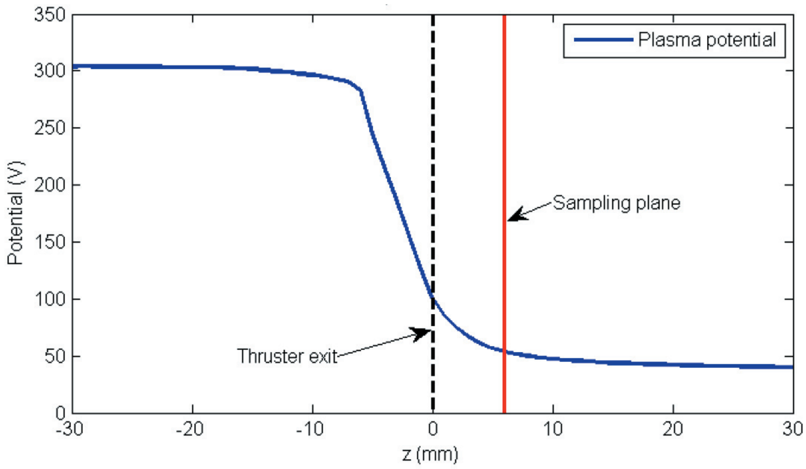

Figure 4: Plasma potential along the acceleration channel and choice of sampling plane.

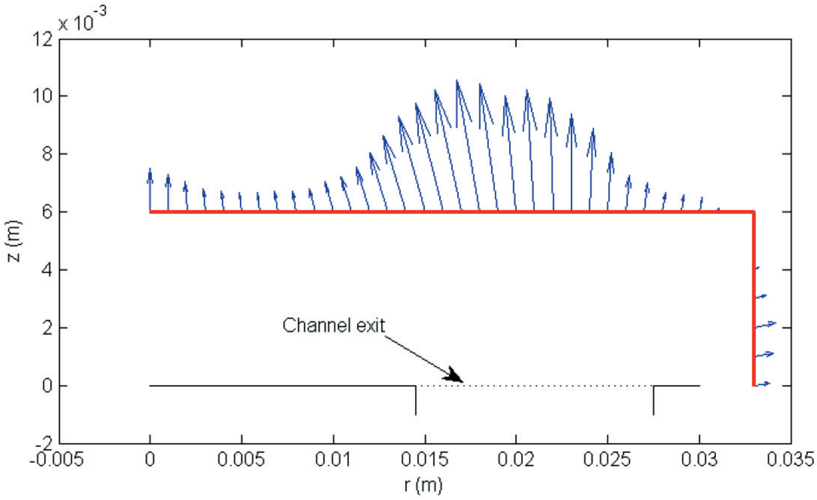

Figure 5: Sampling profile outside thruster exit and ion current density vectors.

n_0, T_{e0}, and ϕ_0 are sampled at $z = 6mm$ and $r = 21mm$, at the channel's centerline. Their values are respectively: $n_0 = 1.918 \times 10^{17} m^{-3}$, $T_{e0} = 6.122eV$, and $\phi_0 = 54.989V$.

The axial component of the ion current is taken from the experimental data, while the radial component is computed using an analytical divergence model based on the magnetic field geometry:[13]

$$\frac{v_r}{v_z} = \frac{a(B_{ri} - B_{rf})}{L\bar{B}_r} \tag{3}$$

Where a is $r - \bar{r}$ with $\bar{r}$ the coordinate of the channel centerline; L is the axial distance of the sampling plane from the ionization region; B_{ri}, B_{rf}, and $\bar{B}_r$ are the radial components of the magnetic field in the ionization area, on the sampling plane, and on average respectively.

The ion temperature is assumed isotropic and is sampled from a precedent fully kinetic PIC simulation of the acceleration channel[4] .

IV. Results

A. Qualitative Results

A general understanding of the effect of the plume crossing can be obtained from observing Figs.6a and 6b, showing the number density profiles before and after the crossing. By comparing the combined with the stand-alone simulations after the crossing (second figure) we can see how the ions tend to stay closer to the centerline, diminishing the overall divergence of the beam.

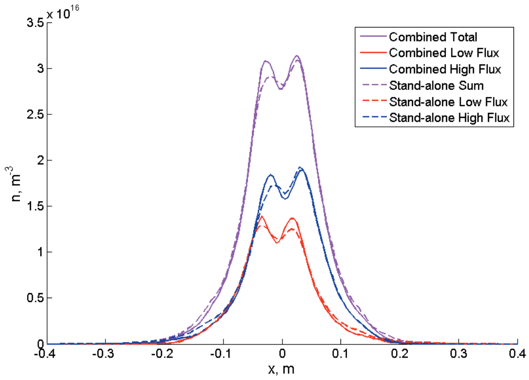

(a) Comparison of number density profiles at $z = 0.25m$, before plume crossing.

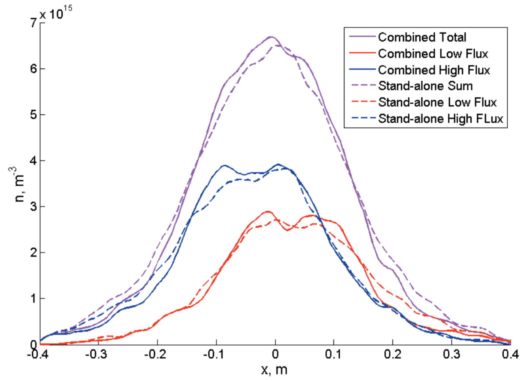

(b) Comparison of number density profiles at $z = 0.5m$, after plume crossing.

It has to be noted that these results are similar to those obtained in a previous work[14] where collisions were not computed. The decrease in divergence then has to be attributed to a deviation of the external layers of the main plume, and note to a mere deflection of the charge-exchange ion wings. Figure 7 shows a qualitative comparison of the testing of our code in a parallel configuration with experimental results obtained by Beal.[15] It can be seen that, despite our model is again not considering collisions, the two distributions present the same trend.

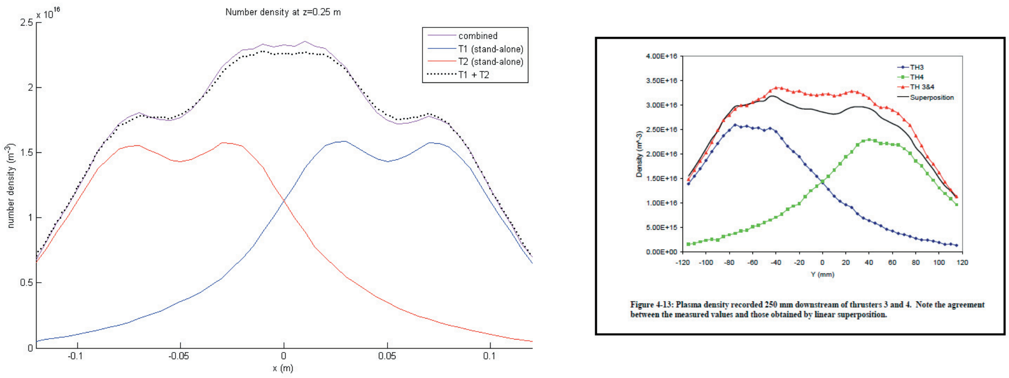

Figure 7: Comparison between numerical (left) and literature experimental (right) data for parallel thrusters.

Going back to our present model, including collisions, Fig.8 shows the comparison of the ion current streamlines in the low flux thruster, in the combined and stand-alone cases. Plume deviation can be clearly seen.

B. Divergence Determination

To give a numerical quantification of the effect of clustering we should rely on the computation of plume divergence. There are two main definitions of the divergence angle: one is the semi-aperture of a cone containing 95% of the total current density, while the other is the arc-cosine of the ratio of the integrals on an hemisphere of the axial and total ion current.

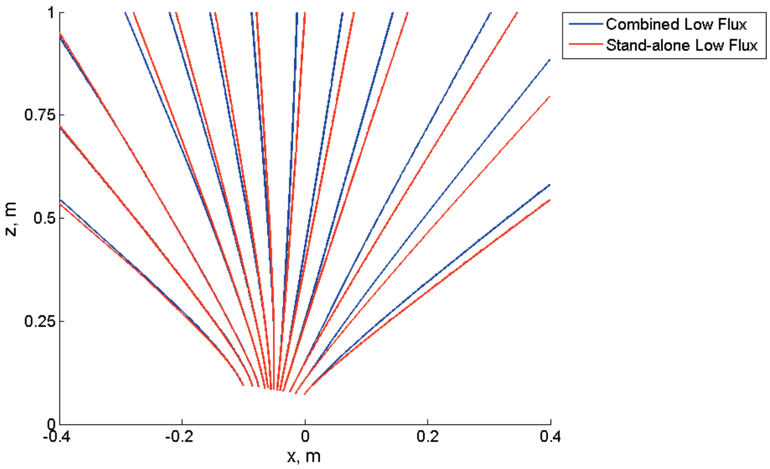

Figure 8: Comparison of the streamlines of ion current relatively to the low-flux thruster for stand-alone and combined simulations.

The first definition focuses on the solid angle influenced by the plume itself, and is more interesting when dealing with interferences caused by the plume and with system integration; the second definition instead is more apt to describe thrust losses caused by divergence. Both these definitions need modifications in the case of a converging thrust-vectoring cluster.

In the first case, it has to be noted that the value of divergence obtained depends on the surface used for sampling the ion current; a hall thruster plume is in fact not conical near the thruster exit. Moreover in the case of a two-thruster cluster the total plume will not be axisymmetric. The proposed solution is then to select a sampling surface, for instance an hemisphere centered in the cluster midpoint, and to measure the ion current distribution on the surface. A current density distribution function can then be derived, and it can be integrated from infinity to the current where the 95% of the total is reached:

$$j_{95} = J | \int_J^\infty P(j)dj = 0.95 \tag{4}$$

Finally, the isovalue contour for $j = j_{95}$ is drawn, and the divergence angle in a direction d can be computed by intersecting the contour with the zd plane. Figure 9 shows the process.

Table 2 shows the divergence angles in the x and y directions for the stand-alone and combined simulations.

Table 2: Directional divergence at $R = 0.4m$ comparison for different thrusters and configurations.

Thruster	Direction X+	Direction X-	Direction Y+	Direction Y-
Stand-alone sum	25.4^o	25.8^o	26.1^o	24.7^o
Stand-alone low flux	27.3^o	22.2^o	26.3^o	25.2^o
Stand-alone high flux	22.3^o	26.8^o	24.8^o	24.5^o
Combined total	23^o	23.8^o	24.8^o	25.4^o
Combined low flux	22.9^o	22.9^o	24.8^o	25.9^o
Combined high flux	23.1^o	25.1^o	25.4^o	24.9^o

It can be noted that not only the total divergence in the combined case is smaller than the stand-alone sum, but also that in the combined case the total divergence is smaller than the one of a single thruster. Figure 10 shows the comparison of divergence contours at $R = 0.4m$ for the combined total and stand-alone sum.

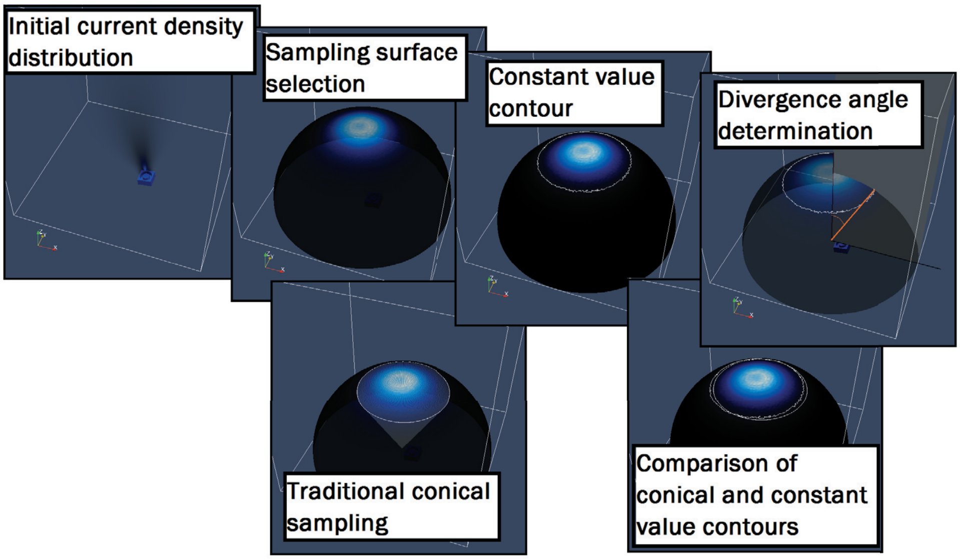

Figure 9: Process for asymmetrical divergence determination and comparison with standard method.

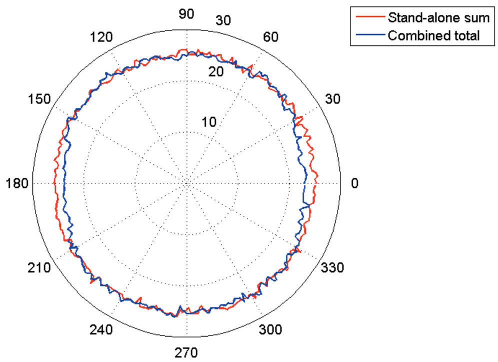

Figure 10: Comparison of polar diagrams for the divergence angle.

In the case of a thrust-vectoring cluster the thrust-oriented divergence is ill defined for single thrusters. A total divergence however can be computed by substituting the z direction in the definition with the direction in which the thrust is directed to.

Table 3 shows the results applying this definition. It has to be noted that, since these calculations are based on ion current, the fast neutrals produced by charge-exchange collisions are not considered.

Table 3: Thrust-related divergence at $R = 0.4m$ comparison.

	Thruster		
Configuration	Sum/Total	Low Flux	High Flux
Stand-alone	19.6^o	20.3^o	19.1^o
Combined	19.1^o	19.6^o	18.7^o

C. Charge Exchange Ion Trajectories

Figure 11 shows the position and velocity of sample charge exchange ions. It is clear how the potential associated with the plume cores is deflecting the slow ions, effectively shielding the areas behind and likely the thrusters themselves. In order to determine the effect of charge-exchange ions on a spacecraft, however, it is necessary to employ a model that includes surface potentials, once the geometry is known.

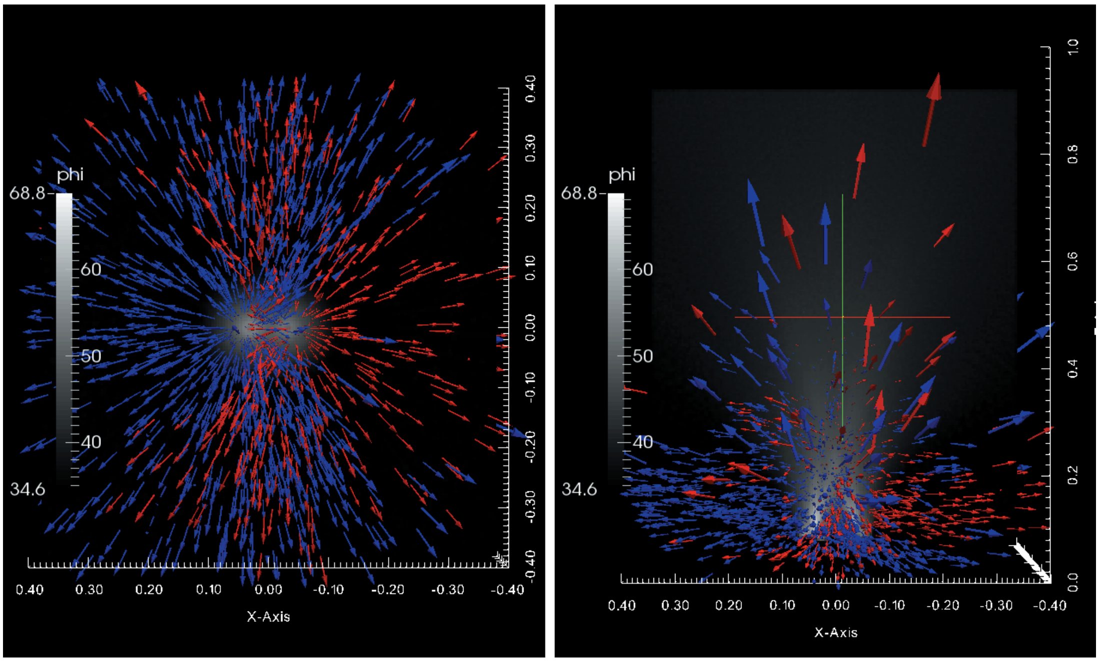

Figure 11: xy and xz projections of charge exchange ions positions and velocities over plasma potential. High flux on the left in blue, low flux on the right in red.

V. Conclusions

This study shows really promising results for the implementation of thrust-vectoring clusters, and encourages further research on the topic.

Interesting directions could be the use of Direct Simulation Monte Carlo collisions in order to better characterize the impact on thrust, the study of surface interactions of charge-exchange ions, and the use of a more refined input for the change of thruster current, that would allow to determine an optimal configuration for thrust-vectoring.

Specific experimental validations are also of course necessary.

Acknowledgments

The authors would like to thank Mr. Crown and the Crown Family Doctoral Fellowship for their generous support.

References

[1]Kapulkin, A. and Guelman, M. "Theoretical modeling of ionization processes in anode cavity of CAMILA Hall thruster," *Presented at the Thirty-First International Electric Propulsion Conference*, Ann Arbor, Michigan, 2009.

[2]M. Guelman, A. Shiryaev, "Cluster of Low Power Electric Thrusters for Communication Satellites", Internal Report, ASRI, Technion, I.I.T., January 2012.

[3]Kronhaus, I., Kapulkin, A., Balabanov, V., Rubanovich, M., Guelman, M., and Natan, B., "Discharge Characterization of the Coaxial Magnetoisolated Longitudinal Anode Hall Thruster," *Journal of Propulsion and Power*, (2013), accessed June 6, 2013.

[4]Kronhaus, I., Kapulkin A., Guelman M., and Natan, B., "Investigation of two discharge configurations in the CAMILA Hall thruster by the particle-in-cell method," *Plasma Sources Science and Technology*, Vol. 21, 2012, p. 035005.

[5]Kronhaus, I., Kapulkin, A., Balabanov, V., Rubanovich, M., Guelman, M., and Natan, B., "Investigation of physical processes in CAMILA Hall thruster using electrical probes," *Journal of Physics D : Applied Physics*, Vol. 45, 2012, p. 175203.

[6]Duchemin, O., Lorand, A., Notarianni, M., Valentian, D., and Chesta, E., "Multi-Channel Hall-Effect Thrusters: Mission Applications and Architecture Trade-Offs," *Presented at the Thirtieth International Electric Propulsion Conference*, Florence, Italy, 2007.

[7]Beal, B. E., Gallimore, A. D., and Hargus, W.A., "The Effects of Clustering Multiple Hall Thrusters on Plasma Plume Properties," *Proceedings of the Thirty-Ninth Joint Propulsion Conference Exhibit*, AIAA, Huntsville, Alabama, 2003.

[8]Walker, M. L. R. and Gallimore, A. D., "Performance Characteristics of a Cluster of 5-kW Laboratory Hall Thrusters," *Journal of Propulsion and Power*, Vol. 23, No. 1, 2007, pp. 35-43.

[9]Celik, M., Santi, M., Cheng, S., Martinez-Sanchez, M., and Peraire, J., "Hybrid-PIC Simulation of a Hall Thruster Plume on an Unstructured Grid with DSMC Collisions," *Presented at the Twenty-Sixth International Electric Propulsion Conference*, Toulouse, France, 2003.

[10]Matthews, A. P., "Current Advance Method and Cyclic Leapfrog for 2D Multispecies Hybrid Plasma Simulations," *Journal of Computational Physics*, Volume 112, Issue 1, pp. 102-116, 1994.

[11]Scharfe, M. K., Koo, J., Azarnia, G., "DSMC Implementation of Experimentally-Based $Xe^{+} + Xe$ Differential Cross Sections for Electric Propulsion Modeling", ERC, Incorporated and Air Force Research Laboratory, Edwards AFB, CA, 93524, 2010.

[12]Huismann, T. D., "Improving Hall Thruster Plume Simulation through Refined Characterization of Near-field Plasma Properties", Ph.D. dissertation, University of Michigan, 2011.

[13]Fruchtman, A., and Cohen-Zur, A., "Plasma lens and plume divergence in the Hall thruster," *Applied Physics Letters* 89, 2006.

[14]Laterza, M., and Guelman, M., "Numerical Modeling of Plume Divergence in a CAMILA Hall Thruster Cluster", *Presented at the Fifty-Fifth Israel Annual Conference on Aerospace Sciences*, Tel Aviv, February 2015.

[15]Beal, B. E.,"Clustering of Hall Effect Thrusters for High-Power Electric Propulsion Applications", Ph.D. dissertation, University of Michigan, 2004.